Temperature dependence of spin fluctuation scattering of neutrons on pyrrhotite

Sz. Kraśnicki, A. Wanic, Ž. Dimitrijević, R. Maglić, V. Marković, J. Todorović

LE JOURNAL DE PHYSIQUE TOME 25, MAI 1964, PAGE 634.

TEMPERATURE DEPENDENCE OF SPIN FLUCTUATION SCATTERING OF NEUTRONS ON PYRRHOTITE (1)

By Sz. KRAŚNICKI, A. WANIC,
Institute of Nuclear Physics, Cracow, Poland.

Ž. DIMITRIJEVIĆ, R. MAGLIĆ, V. MARKOVIĆ, J. TODOROVIĆ,
Institute for Nuclear Sciences, Vinča, Yugoslavia.

Résumé. — A l'aide du spectromètre à neutrons triple axe de Cracovie installé à Vinca (Yougoslavie), la diffusion cohérente inélastique des neutrons de longueur d'onde $\lambda = 1{,}376$ Å liée au point $\boldsymbol{\tau} = (001)$ a été étudiée à différentes températures jusqu'à 400 °C, c'est-à-dire, bien au-dessus de la température critique ($T_N = 320$ °C).

L'intensité du cône de diffusion (001), augmente avec la température, mais son caractère « magnon » reste sans changement. Néanmoins, à partir de 200 °C, les raies « magnons » commencent à s'élargir. Cette température n'est pas très sensible à l'énergie d'un groupe de magnons donnés. Le degré élevé d'inélasticité se maintient au-dessus de la température critique, et le transfert moyen d'énergie reste très voisin de celui à basse température. Les résultats sont discutés en fonction de la durée de vie des magnons et de l'effet de la température sur le couplage d'échange effectif.

Abstract. — By means of the triple axis Cracow neutron spectrometer installed at Vinca (Yugoslavia), coherent inelastic scattering of monochromatic neutrons ($\lambda_0 = 1.376$ Å) connected with $\boldsymbol{\tau} = (001)$ was investigated at various temperatures above room temperature up to 400 °C, i.e. above the critical point ($T_N = 320$ °C) of the spin alignment in pyrrhotite. The intensity of the (001) scattering cone increases with temperature but its magnon character does not change. Only at temperatures above 200 °C do the widths of the magnon peaks begin to increase. This temperature is not very sensitive to the energy of a given magnon group. The high degree of inelasticity is maintained over the critical point region and the mean energy transfer is close to the one for low temperatures. The results are discussed in terms of magnon lifetime and temperature dependence of effective exchange coupling.

I. Introduction. — While the magnetic inelastic scattering of neutrons sufficiently below the critical point of spin alignment in crystals is well described by existing theories, this cannot be said with certainty of the situation arising in the vicinity of the critical point.

For lower temperatures the scattering can be analysed applying directly spin wave theory as mentioned in [15]. At temperatures near the critical point the spin wave approximation loses its validity and the more general formalism, invented by Van Hove [14], has to be introduced, describing the system by time dependent spin correlation functions. Neutron scattering cross-sections are their integral transforms. Thus the problem was reduced to finding the expressions for spin correlation functions. At low temperature they can be related with spin wave theory and give the same picture [3], [14]. In the critical region their behaviour is represented in terms of r_1, $\varkappa_1$, Λ_1 parameters introduced by Van Hove [14] and discussed by others authors [2], [3], [9] as well as measured in a number of neutron scattering experiments [6], [10], [13].

Crucial in the problem is the inelasticity of scat-

(1) This work was carried out as one of the joint projects based on Polish-Yugoslavian agreement on cooperation in science and financed by the Federal Nuclear Energy Commission of Yugoslavia and the Polish Governement Commission for the Use of Nuclear Energy.

tering connected with the magnitude of the spin diffusion constant Λ_1. It was believed that Λ_1 is zero at the critical point making the scattering elastic. However, recent neutron investigations [6], [11] do not seem to corroborate this opinion. Hence it was interesting to extend the measurements described in [15] to the region of higher temperatures.

II. **Measurements.** — Measurements were performed in Vinca by a technique essentially the same as that described in [15], using the Cracow Neutron Spectrometer and the same crystal of pyrrhotine. For this reason the description of many details which can be found in [15] will not be repeated.

The crystal sample was placed in a furnace (see *fig.* 1) mounted not on the goniometer head but on a special plate with an adjustable position. This plate could be fixed on the axis of any spectrometer table, and the position of the furnace properly adjusted. The temperature inside the furnace was measured by a device controling the voltage applied to the heating wire.

The measurements of the magnetic scattering were carried out both by the diffraction and the energy analysing techniques using the same wave length ($\lambda_0 = 1{,}376$ Å) of incident neutrons.

The angular distribution of intensity within the cone of scattered neutrons connected with $\tau = (00.1)$ was investigated at a number of different temperatures for five missetting angles 7,5°, 15°, 23°, 33°, and 41°. Some of the obtained curves are represented in figures 2 and 3.

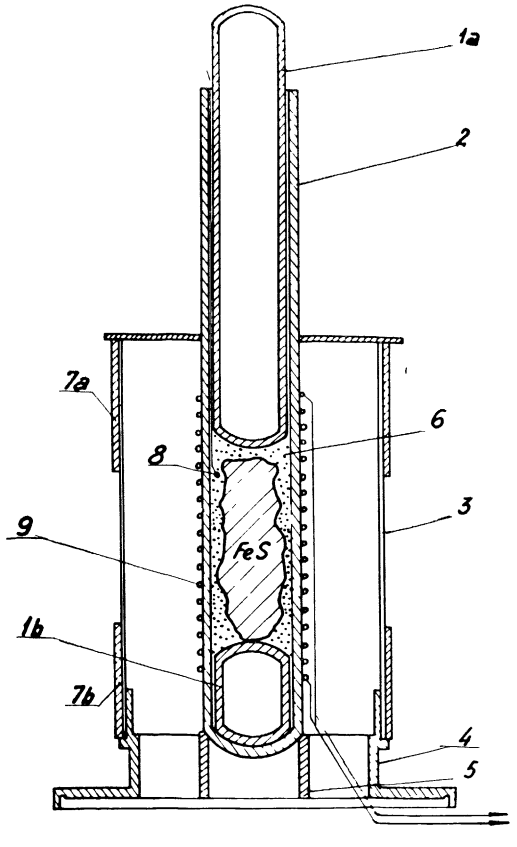

FIG. 1. — Scheme of the furnace for the pyrrhotite sample : 1*a*) and b-glass cylinders. — 2) Quartz cylinder. — 3) Aluminium shielding for thermal radiation. — 4) Aluminium device for keeping 3 fixed to positioning plate. — 5) Ceramic isolator also fixed to positioning plate. — 6) Aluminium powder. — 7*a*) and b-cadmium shieldings. — 8. Thermocouple. — 9. Heating wire.

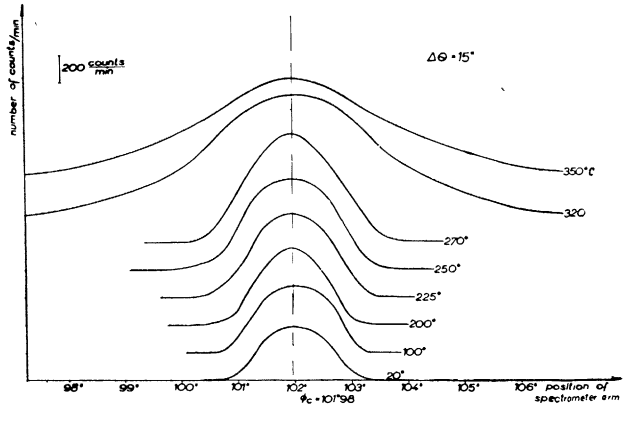

FIG. 2. — Family of diffraction curves for $\Delta\theta = 15°$ and for different temperatures. Background was subtracted and curves drawn aside in the vertical direction with unit of the scale constant : φ_c = theoretical position of the centre of the peaks.

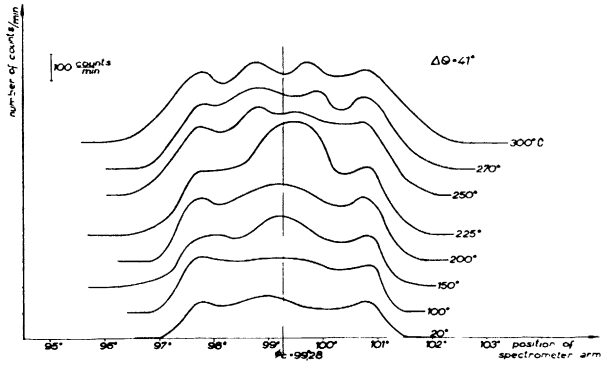

FIG. 3. — Family of diffraction curves for $\Delta\theta = 41°$ and for different temperatures.

For the energy analysis two methods of observations were used. At first for $\Delta\Theta = 23°$ the conventional way of analysing was applied but without collimation in the vertical plane usually applied between the sample (placed on table II) and the analyser (Zn-crystal placed on table I). At this missetting angle the instrumental reso-

lution was sufficient for the separation of intensities from the magnon and elastic scattering at room temperature. Thus the situation in reciprocal space discussed in [10] (see *fig.* 2 of [10]) could be studied. The curves obtained in this way can be seen in figure 4.

They directly show that the diffuse peaks observed by diffraction technique should be entirely ascribed to inelastic scattering in the whole temperature range.

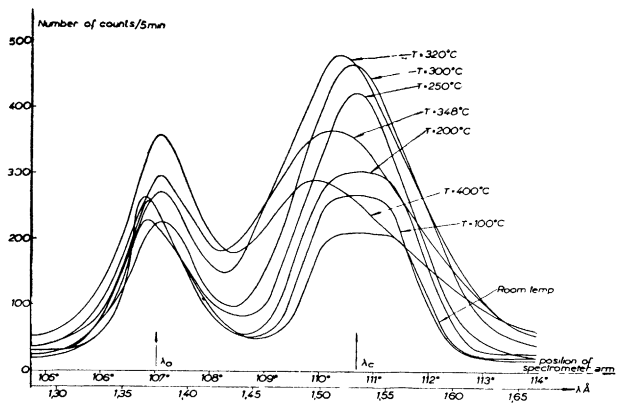

FIG. 4. — Family of curves obtained by the conventional energy analysing method at various temperatures (T_N = 320 °C) for $\Delta\theta$ = 23° ($E_{spin\ wave}$ = 8,1 meV) without additional collimation in the vertical plane :

λ_0 : theoretical position of the centre of the elastic peak.

λ_c : theoretical position of the centre of the inelastic peak.

In order to check this inference for other energies (missetting angles) another method was used, i.e the intensity of scattered neutrons was recorded at constant energy and momentum transfer, by setting the analyser (Zn-crystal and detector) in a predetermined fixed position. This position was chosen in such a way that the detecting spot in reciprocal space (in laboratory frame) was centered around the point which corresponded to the end of the τ-vector when the crystal sample was misaligned by a given angle $\Delta\Theta_c$.

The number N of detected neutrons was then recorded for different positions $\Delta\Theta$ of the sample when it was rotated in steps around the vertical axis. For $\Delta\Theta$ close to $\Delta\Theta_c$ the corresponding fragment of the scattering surface entered the detecting spot and the counting rate increased. On theoretical grounds the spectra should exhibit left and right symmetry around $\Delta\Theta_c$, which was roughly observed (therefore curves on figure 5 are symmetrised).

An important advantage of the method is the constancy of the analysing system efficiency. This is not fulfilled when the detecting spot is caused to wander because of the Renninger effect in the analysing crystal. $(\Delta\Theta - \Delta\Theta_c)$ directly gives the q-value because $q = \tau|\Delta\Theta - \Delta\Theta_c|$ for not too high $|\Delta\Theta - \Delta\Theta_c|$.

The measurements were performed at various temperatures of the sample for two different energy transfers ΔE equal 13 meV and 16,5 meV which correspond to $\Delta\Theta_c$ equal 41° and 59° respectively. The vertical collimation used was respectively 1°

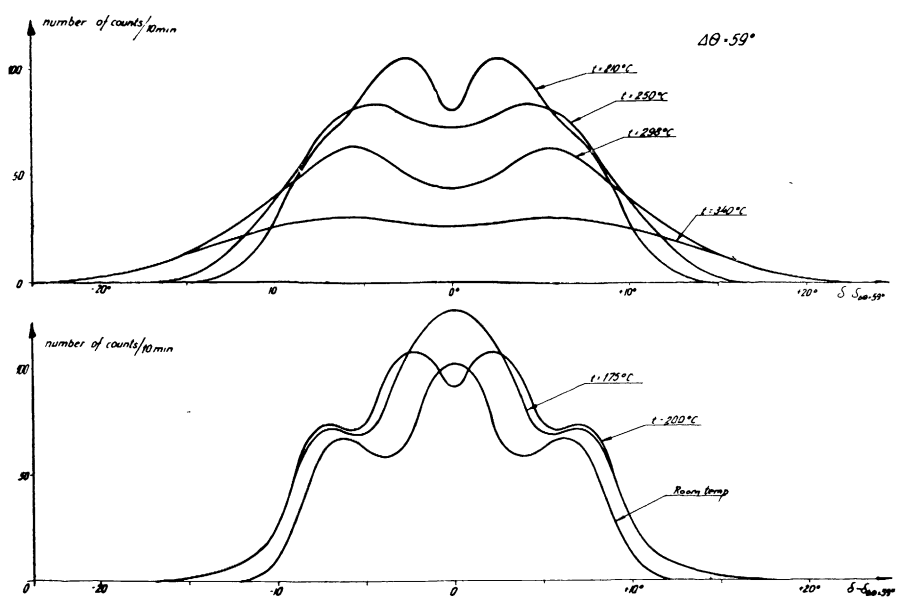

FIG. 5. — Family of curves obtained by the constant energy transfer method at various temperatures for position of the analysing spot lying around the end of the vector τ for $\Delta\theta_c$ = 59° — subtraction of the background and symmetrisation procedures were applied.

and 1,5°. The family of curves of $\Delta\Theta_c = 59°$ is represented in figure 5.

III. **Analysis of the results.** — The results were analysed under the assumption of the existence of collective motion excitations in the whole investigated region of temperatures, which at lower temperatures were identified with magnons. This point of view has recently obtained some theoretical [7], [8] as well as experimental [11] support.

However, it should be noted that the experiments could not distinguish contributions from transverse and longitudinal spin fluctuations [10]. Thus it had to be assumed for the purpose of practical elaboration of the results that the excitations are of a single type and possess a certain dispersion relation $\hbar\omega(q)$ (defined for the centre of ω_q-distribution) together with an energy width γ of the " magnon " lines [5], [11]. Then the observed diffuse scattering peaks in an energy interval $\Delta(\hbar\omega)$ should depend on two parameters : effective exchange energy (if the form of the dispersion curve is conserved) and energy width γ. Approximate calculations, explained in the appendix, made it possible to obtain the temperature dependence and to estimate the numerical values of these parameters. The energy width can be related to the excitation life time $\tau = \hbar/\gamma$.

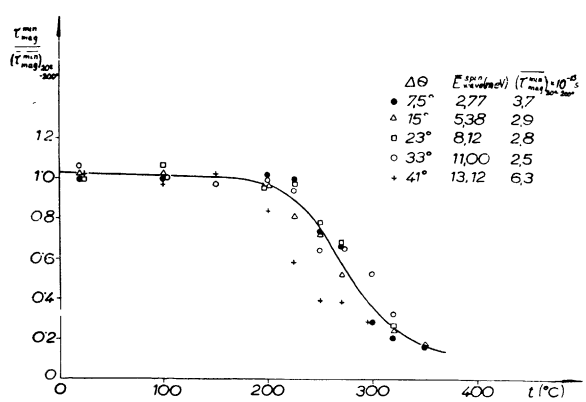

FIG. 6. — The temperature dependence of the lower limits τ_{mag}^{min} of the magnon life times obtained under the assumption of constant instrumental width equal the width of the Bragg reflection peak. Results are represented in the units equal to $(\overline{\tau_{mag}^{min}})_{20°-200°}$ which are tabulated in the figure : $(\overline{\tau_{mag}^{min}})_{20°-200°}$ = average values τ_{mag}^{min} obtained for the temperatures between 20 °C and 200 °C.

The differences $\Delta\Gamma$ between the width at half of the peak height and the width defined by slopes of the peak wings, obtained as a result of the analysis of diffusion curves, show evident deviations from the half width of the instrumental resolution function. From these broadenings lower values of magnon life times can be calculated. They are confronted in figure 6. But because the applied instrumental curve (Bragg peak profile) is only an approximation, the lower temperature values of $\Delta\Gamma$ can be taken as representing the real instrumental width, although depending on missetting angle. Life times derived under this assumption are presented in figure 7. Figure 8 and 9 show respectively temperature dependences of $\Gamma_{1/2h}$ and effective exchange energies I_1 derived from them (maintaining the form of the dispersion law [15]).

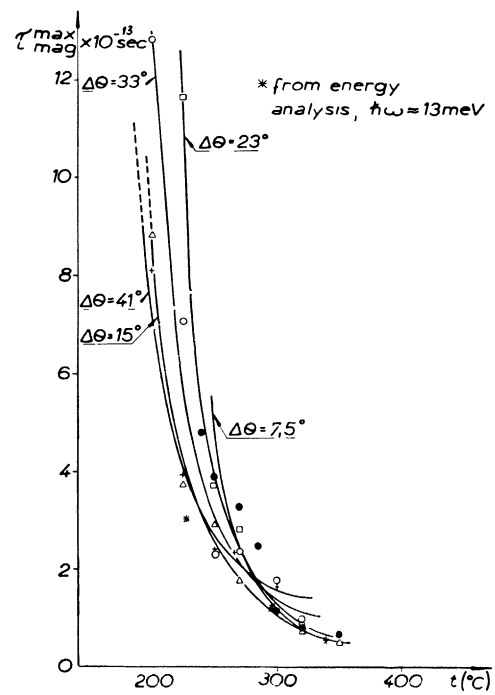

FIG. 7. — The temperature dependence of the upper limits τ_{mag}^{max} of the magnon life times obtained under assumption that the observed differences $\Delta\Gamma$ at lower temperatures provided the real instrumental widths for different missetting angles.

The curves obtained by the constant energy transfer method (*fig.* 5) are not very suitable for elaboration because of low instrumental resolution and existence of the central peak (it was ascribed [15] to the optical mode and as can be inferred from figure 5 the character of the temperature dependence of this mode is more rapid then for the acoustic one). In order to obtain information about the magnon life times the analysis of slopes was preferred so as to avoid the influence of the central maxima (the presence of which disturbed for large $\Delta\theta$ the picture of the acoustic ones).

The slope of the curve obtained at room temperature was taken as corresponding to excitations with infinite life times. The changes in slope could then be considered as caused by line broa-

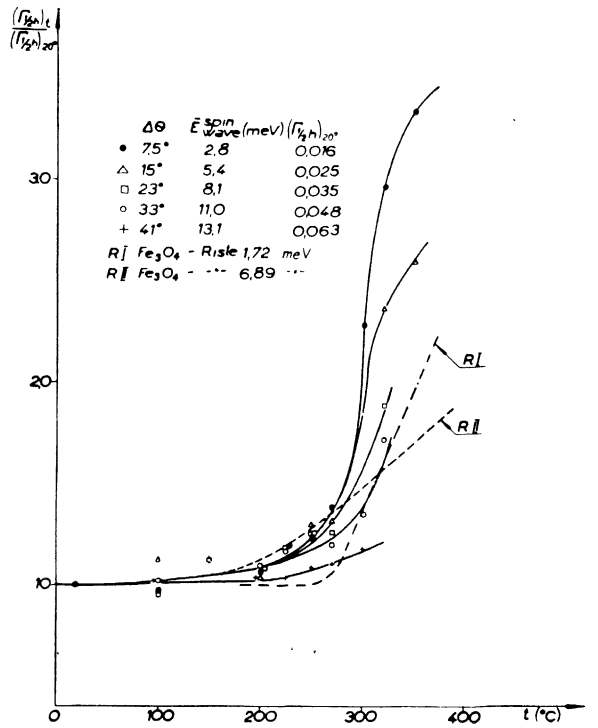

FIG. 8. — The temperature dependence of the $\Gamma_{1/2\hbar}$ widths for different missettings. Curves normalized to unity at room temperature. Curves denoted by R I and R II are obtained from curves represented in reference [11] by reduction of the temperatures by a factor

$$(\overline{T_N})_{FeS}/(T_C)_{Fe_3O_4}.$$

dening. When the q (wave vector) distribution at constant ω was taken as gaussian, the diminution of the slope could easily be connected with γ. The values of life times deduced in this way from these curves (for $\Delta\theta_c = 41°$) are presented in figure 7.

One of the curves for $\Delta\theta_c = 59°$, above the critical point, was compared with the theoretical distribution given by the Van Hove's [14] formula, reduced to the form :

$$\frac{dN}{dq\, d\omega} \simeq \frac{\text{const.}}{\varkappa_1^2 + (2\pi q)^2} \frac{\Lambda_1(2\pi q)^2}{\omega^2 + \Lambda_1^2(2\pi q)^4} \qquad (1)$$

where weak terms have been neglected.

As can be seen from fig. 10, the character of the peak is more or less satisfactorily reproduced. Unfortunately the correction for resolution cannot be performed with reliable accuracy. However, the distortion of the form of the wings should not be so serious as in the central part of the distribution. The comparison of the curves in figure 10 leads to the estimate : $\Lambda_1 = (40 \pm 10) \times 10^{-3}$ c. g. s. units and $x_1 \leqslant 1 \times 10^{-2}$ Å^{-1}.

In order to find how the temperature changes the intensity of a different excitation group, the areas under the diffuse peaks (see for instance

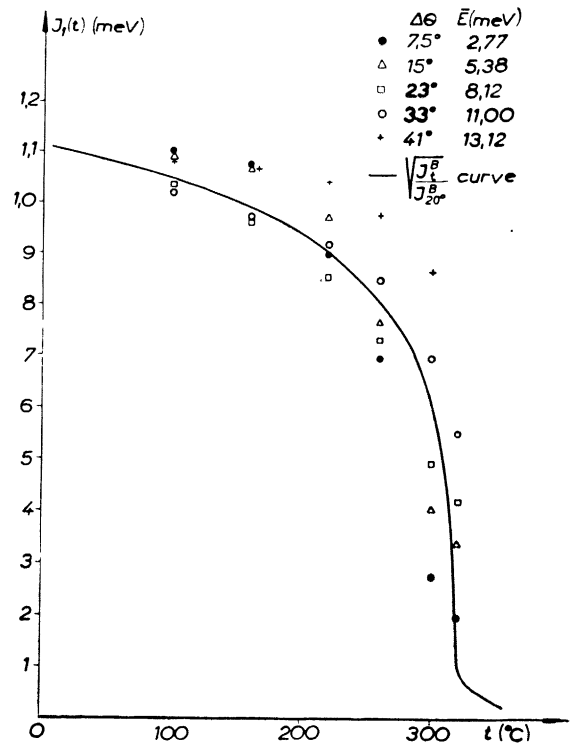

FIG. 9. — The temperature dependence of the exchange stiffness I_1. Points for different missettings were calculated under the assumption of the validity of the dispersion law — see reference [15]. Values of $\Gamma_{1/2\hbar}$ were taken from curves represented in figure 8. At room temperature all points are normalized to $I_1 = 1{,}1$ meV. The solid line shows the changes of square root of the relative intensity of Bragg reflection.

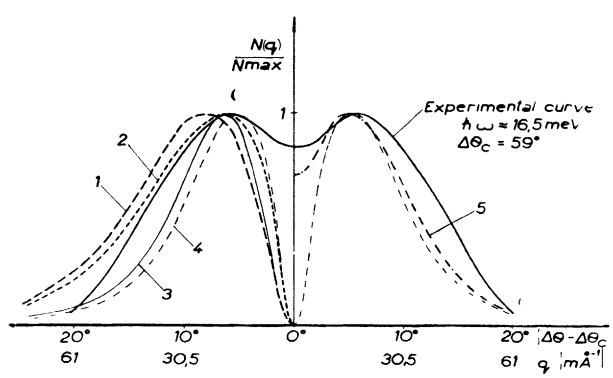

FIG. 10. — The comparison of the observed peak (T = 340 °C — see fig. 5) profile with the profiles given by formula (1) for different x_1 and Λ_1 :

1. $x_1 = 1{,}2 \times 10^{-2}$ Å^{-1} $\Lambda_1 = 6{,}8 \times 10^{-2}$ cm^2/s
2. $x_1 = 0{,}6 \times 10^{-2}$ Å^{-1} $\Lambda_1 = 6{,}8 \times 10^{-2}$ cm^2/s
3. $x_1 = 1{,}2 \times 10^{-2}$ Å^{-1} $\Lambda_1 = 3{,}4 \times 10^{-2}$ cm^2/s
4. $x_1 = 0{,}6 \times 10^{-2}$ Å^{-1} $\Lambda_1 = 3{,}4 \times 10^{-2}$ cm^2/s
5. The curve 4 modified by roughly estimated instrumental resolution.

fig. 2) were integrated. These are presented in figure 11. The theoretical curve seen in the same figure was calculated from the approximate formula :

$$\frac{J_t}{J_0} \simeq \frac{(e^{\hbar\omega/kT_0} - 1)\, e^{\hbar\omega/kT}}{(e^{\hbar\omega/kT} - 1)\, e^{\hbar\omega/kT_0}} \cdot (\Gamma_t/\Gamma_0)^2 \qquad (2)$$

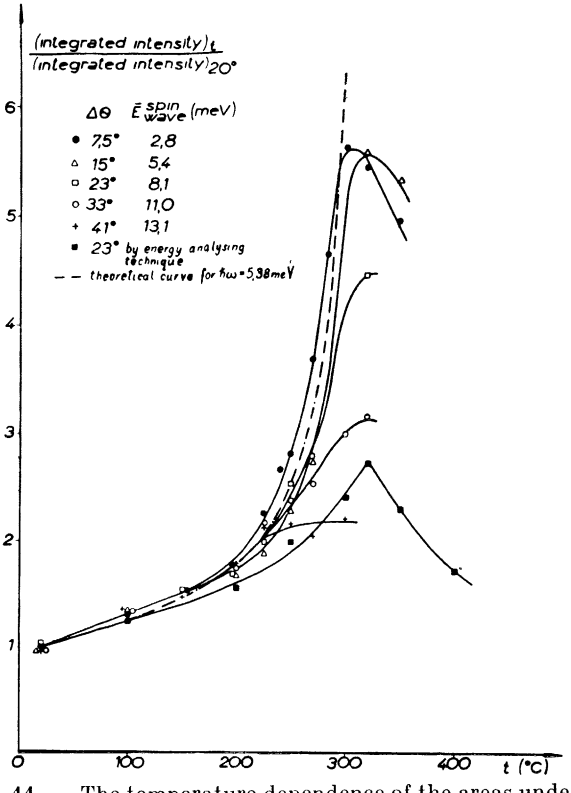

FIG. 11. — The temperature dependence of the areas under the diffuse peaks for different missettings. Experimental points denoted by black squares were obtained from curves represented in figure 4 (only the inelastic part was taken). The theoretical curve for $\Delta\theta = 15°$ was calculated from formula (2).

taking into account the observed temperature variation of $\Gamma_{1/2h}$ (see *fig.* 8) and the Bose-Einstein population factor.

There are also marked points obtained for $\Delta\theta = 23°$ (see *fig.* 4) by the energy analysing technique. Of course they cannot give the same dependence as that observed by the diffraction technique because of the peak widening. However, the discrepancy has the expected sign.

IV. **Discussion of the results.** — The qualitative behaviour of the scattering when the temperature changes appears to be identical as in other magnetics — Fe_3O_4 [12], Fe_2O_3 [13], Fe [6] so far investigated. For a general discussion of the effects the reader is referred to [10]. Because of the lack of any firm theoretical basis which could be applied to the case under investigation, the discussion must be limited to a comparison with the results obtained for Fe_3O_4, for which the largest amount of data has been assembled by other experimental works [1], [12], [11].

It is interesting to note that in pyrrhotite the life times of excitations are about an order of magnitude smaller than in Fe_3O_4. These are the only two substances where they have been estimated.

The point in which the parameters of the unperturbed magnon picture of the scattering begin to exhibit distorsion (200 °C) — see figures 6, 8, 9, and 11 — is roughly the same (when expressed in the reduced temperature — T/T_C) as in Fe_3O_4 [11] but seems rather independent of the q-value or effective energy of the magnon group. The effective exchange stiffness (1) behaves roughly as the magnetization but certainly does not vanish in the critical point. This could be interpreted in favour of the concepts which extend the magnon or collective excitation picture to or even above the critical point [4], [7], [8]. However, it is better to say at present that the results for pyrrhotite reveal with certainty only the fact that in the investigated region of q-values the scattering does not lose its inelastic character even for temperatures close to the critical point.

It can be noted that the appearance of the observed inelastic scattering peaks is not in radical contradiction to the ones foreseen by the Van Hove treatment (formula (1)) based on the spin diffusion approximation and valid only in the limit of small q values. Recently Mori and Kawasaki [9] pointed out that the damping constant for longitudinal spin fluctuations can have a term (strongly q dependent) which does not vanish at T_C.

V. **Acknowledgements.** — The authors would like to express their sincere gratitude to Professor F. Boreli of the " Boris Kidrič " Institute for Nuclear Sciences and Professors H. Niewodniczański and J. Janik of the Cracow Institute for Nuclear Physics for their kind support and encouragement.

VI. **Appendix.** — One has to isolate the theoretical shape from the convolution of the ideal diffuse peak with the instrumental resolution function. The latter was taken in the two following forms :

$$T_{in}(\alpha) = \begin{cases} 0 & \text{for} \quad \alpha \geqslant \Gamma_0/2 \\ -\dfrac{2B}{\Gamma_0}\alpha + B & 0 \leqslant \alpha \leqslant \Gamma_0/2 \\ & \text{the triangle form} \\ +\dfrac{2B}{\Gamma_0}\alpha + B & -\Gamma_0/2 \leqslant \alpha \leqslant 0 \\ 0 & \alpha \leqslant -\Gamma_0/2 \end{cases} \qquad (A1)$$

$$T_{in}(\alpha) = B.exp\left\{-(2\alpha/\Gamma_0)^2\right\} \quad \text{the gaussian form} \qquad (A1')$$

(1) Under the term " exchang stiffness " we understand the product $J_1.(S_a - S_b)$, see [15].

where α = angle between the axis of the collimator and direction of the neutron propagation,
B = constant of proportionality,
Γ_0 = total width of the resolution function,
$\bar{\Gamma}_0 = \Gamma_0/(2\sqrt{\ln 2})$.

Because the array of counter w'th a wide detection angle in the vertical plane was used, it can be assumed that automatic integration of the intensity in this direction took place.

When the natural width of magnon lines is neglected, it was proved by means of numerical integration that the quasi δ-shape (on the edges) angular distribution (see *fig.* A1-*a*) is transformed to a nearly rectangular one $I_p(\alpha)$ (this is valid for a not too high angular resolution) — see figure A1-*b*. If the width of the primary distribution $I_p(\alpha)$ is denoted by $2\alpha_0 = \Gamma_{mag}^{real}$ and the height by A, then the convolution of $I_p(\alpha)$ with $T_{in}(\alpha)$-(A1) for the case $\alpha_0 > \Gamma_0/2$ gives the curve (A2) — see figure A1-*c* :

$$I(\alpha) = \begin{cases} 0 \\ \dfrac{A.B}{\Gamma_0}\cdot\left[\alpha - \left(\alpha_0 + \dfrac{\Gamma_0}{2}\right)\right]^2 \\ \dfrac{A.B}{\Gamma_0}\cdot\left\{\dfrac{\Gamma_0^2}{2} - \left[\alpha - \left(\alpha_0 - \dfrac{\Gamma_0}{2}\right)\right]^2\right\} \\ \dfrac{A.B}{2}\cdot\Gamma_0 \end{cases}$$

for respectively

$$\begin{aligned} &\alpha \geqslant \alpha_0 + (\Gamma_0/2) \\ &\alpha_0 \leqslant \alpha \leqslant \alpha_0 + (\Gamma_0/2) \\ &\alpha_0 - \Gamma_0/2 \leqslant \alpha \leqslant \alpha_0 \\ &0 \leqslant \alpha \leqslant \alpha_0 - (\Gamma_0/2) \end{aligned} \qquad \text{(A2)}$$

$$I(-\alpha) = I(\alpha).$$

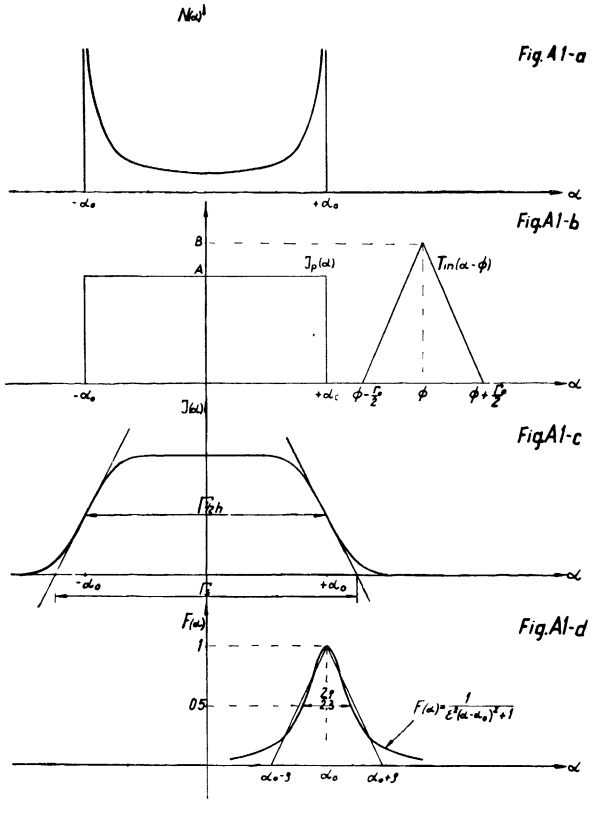

FIG. A1. — Curves explaining the approximate analysis of the diffuse peaks.
a) Theoretical distribution of the intensity in the case of scanning of the magnon cone with ideal resolution in the horizontal plane and good but not ideal resolution in the vertical direction.
b) Assumed theoretical distribution of the intensity $I_p(\alpha)$ of the scanned magnon cone (primary distribution) with practically ideal resolution in the horizontal plane, but with integration in a vertical direction and the instrumental resolution curve used for convolution, $T_{in}(\alpha - \emptyset)$.
c) Distribution of the intensity obtained by the convolution of the two curves represented in figire A1-*b*.
d) Theoretical curve of the angular broadening of the magnon line caused by the definite magnon life time and the triangular approximation used in the calculation.

It is easily seen that the widths $\Gamma_{1/2h}$ at half of the peak height are equal $2\alpha_0$ and that the tangent to the curve at this point cuts off on the abscissa axis the section Γ_s which differs from $\Gamma_{1/2h}$ by $\Delta\Gamma = \Gamma_s - \Gamma_{1/2h}$ where

$$\Delta\Gamma = \Gamma_0/2. \qquad \text{(A3)}$$

Taking into account the natural width of magnon lines γ, the resulting $I_p(\alpha)$ can be approximated by summing many rectangular distributions with heights changing as a certain probability function $F(x)$. This means $I_p(\alpha)$ is given by (A4) :

$$I_p(\alpha) = C\int_\alpha^\infty F(x)\,dx \qquad \text{(A4)}$$

$$I_p(-\alpha) = I_p(\alpha)$$

where C is a constant of proportionality. A Lorentz form (A6) of the function $F(x)$, strictly valid for a linear dispersion law (A5), was assumed :

$$\omega(q) = a + m.q \qquad \text{(A5)}$$

$$F(x) = [\varepsilon^2(x - \alpha_0)^2 + 1]^{-1} \qquad \text{(A6)}$$

where

$$\varepsilon = m \times k_c/\gamma \quad k_c \text{ — see [15].} \qquad \text{(A7)}$$

For the purpose of calculation the $F(x)$ function was replaced by the triangular shape function — see figure A1-*d* — with total width 2ρ equal $4{,}6/\varepsilon$.

Under the above-mentioned assumptions and condition $\alpha_0 > \rho$ the primary distribution $I_p(\alpha)$ has wings, being a quadratic function of the angle, and after convolution with (A1′) the effective $I(\alpha)$

distribution is at first sight similar to (A2), but with $\Delta\Gamma$ given by (A8) :

$$\Delta\Gamma = \frac{\Gamma_0}{2} \cdot \frac{\lambda^2}{\sqrt{\pi} \times \lambda \times \operatorname{erf} \lambda + e^{-\lambda^2} - 1} \qquad \text{(A8)}$$

where

$$\lambda = 4\sqrt{\ln 2} \times (\rho / \Gamma_0). \qquad \text{(A9)}$$

It can be shown that $\Delta\Gamma \to \Gamma_0/2$ for $\lambda \to 0$ and $\Delta\Gamma \to \frac{\Gamma_0}{2} \cdot \frac{\lambda}{\sqrt{\pi}}$ for $\lambda \to \infty$.

So the dispersion law can be measured directly from (A8) and the magnon life time from (A10) :

$$\tau_{mag} \underline{\underline{df}} \, \hbar / \gamma = 9{,}2 \cdot \sqrt{\ln 2} \cdot \hbar / (m \cdot k_c \cdot \Gamma_0 \cdot \lambda). \qquad \text{(A10)}$$

REFERENCES

[1] Brockhouse (B. N.) and Watanabe (H.) ,, Inelastic Scattering of Neutron in Solids and Liquids ", II, p. 297, IAEA, Vienna, 1963.

[2] de Gennes (P. G.), *J. Phys. Chem. Solids*, 1958, **6**, 43.

[3] de Gennes (P. G.) and Villain (J.), *J. Phys. Chem. Solids*, 1960, **13**, 10.

[4] Ginzburg (V. L.) and Fain (V. M.), *Zh. Ekspe Teor. Fiz.*, 1960, **39**, 1323.

[5] Izyumov (J. A.), *Usp. Fiz. Nauk*, 1963, **80**, 41.

[6] Jacrot (B.), Konstantinović (J.), Parette (G.) and Cribier (D.), " Inelastic Scattering of Neutrons in Solids and Liquids ", II, p. 317, IAEA, Vienna, 1963.

[7] Keffer (F.) and London (R.), *J. Appl. Physics*, 1961, **32**, 2S.

[8] Mori (H.), *Prog. Theor. Physics*, 1963, **29**, 156.

[9] Mori (H.) and Kawasaki (K.), *Prog. Theor. Physics*, 1962, **27**, 529.

[10] Riste (T.), *J. Phys. Chem. Solids*, 1961, **17**, 308.

[11] Riste (T.), *J. Phys. Soc.*, Japan, 1962, **17**, SBIII, 60.

[12] Riste (T.), Blinowski (K.) and Janik (J.), *J. Phys. Chem. Solids*, 1959, **9**, 153.

[13] Riste (T.) and Wanic (A.), *J. Phys. Chem. Solids*, 1961, **17**, 318.

[14] Van Hove (L.), *Phys. Rev.*, 1954, **95**, 1374.

[15] Wanic (A.), *J. Physique* (mémoire précédent, p. 627).